Journal of Nuclear Materials 390–391 (2009) 444–447

Contents lists available at ScienceDirect

Journal of Nuclear Materials

journal homepage: www.elsevier.com/locate/jnucmat

Edge turbulence scaling in RFX-mod as measured using GPI diagnostic

P. Scarin *, M. Agostini, R. Cavazzana, F. Sattin, G. Serianni, M. Spolaore, N. Vianello

Consorzio RFX, Associazione EURATOM-ENEA sulla Fusione, Corso Stati Uniti 4, Padova, Italy

ARTICLE INFO

PACS:
52.35.Qz
52.35.Mw
52.35.Ra
52.25.Gj

ABSTRACT

The nature of plasma edge turbulence has been studied in the Reversed Field Pinch (RFP) RFX-mod, making use of a Gas Puffing Imaging (GPI) diagnostic, with high time (2 MHz) and space (5 mm) resolution. The edge turbulence has been characterized in terms of toroidal phase velocity of fluctuations, v_ϕ, of the width of emission structures, 2σ, and of their linear density in the toroidal direction. The packing fraction f_p of intermittent structures has been estimated as the fraction of occupied area in a plane perpendicular to the magnetic field. The behaviors of v_ϕ, f_p, and 2σ are reported as functions of the density normalized to its Greenwald value, n/n_G. A comparison at different plasma regimes of an effective diffusion coefficient D_p due to the plasma trapped in coherent structures has been discussed. A decreasing trend of D_p with n/n_G values has been guessed.

1. Introduction

Edge turbulence has a crucial influence on the performance of fusion devices because it determines the amount of interaction between the plasma and the first wall.

The edge cross-field transport affects the location and the strength of the particle flux to the wall, the processes of recycling and the impurity influx [1]. The edge plasma also sets the conditions for the overall plasma operation either through the formation of edge pressure gradient [2], of radial electric field and velocity shear, or by developing the mechanisms that ultimately lead to the density limit [3,4]. In this context it is important to study the behavior of the turbulence at different plasma regimes. A useful global scaling parameter, to this purpose, is the average electron density normalized to Greenwald density n/n_G [5,6].

Despite the widely different magnetic structure, it has been known for some time that Reversed Field Pinches (RFPs), Tokamaks and Stellarators do share most of the same edge behaviour. A common finding is that various diagnostics of edge plasma in different devices observe intermittent bursts emerging from the background uncorrelated turbulence. This hints to the simultaneous presence of two different driving mechanisms: one for the events detected as coherent structures (blobs) and another for the Gaussian background turbulence [7]. Particle transport driven by coherent structures may amount up to 50–70% of the total for $n/n_G \geqslant 0.3$ [5,8].

The RFP is a self-organized system where the plasma produces, through a dynamo mechanism, involving some level of self-generated non-axis-symmetric magnetic perturbations, its own equilibrium characterized by a toroidal component of magnetic field reversed at the edge with respect to the centre [9]. A reversal parameter $F = B_\phi(\text{wall})/\langle B_\phi \rangle$ is commonly adopted to characterize the RFP equilibrium; F is simply related to the magnetic pitch at the wall.

The RFX-mod device (major radius $R = 2$ m, minor radius $a = 0.46$ m) is presently the largest RFP machine. A rich and flexible feed-back control system provides an almost toroidally symmetric flux surface around the plasma [10]. The data presented in this work are taken in discharges with plasma current $I_\phi = 0.3$–1.1 MA, corresponding to 10–30 MW of ohmic input power, with an average electron density range of $0.5–6 \cdot 10^{19}$ m^{-3}. Core electron temperature ranges between 200 and 500 eV (with records up and above 1 keV at higher plasma current and low n/n_G) and pulse lengths are up to 0.35 s. One of the parameters that affect the edge turbulence in RFP devices is the local distance λ_w (function of the angle ϕ, θ) between the last closed magnetic surface and the wall [11], which quantifies the local plasma deformation. Its value is negative when there is a gap between the well-confined plasma and the wall.

To study the dynamical structures of plasma edge turbulence a GPI diagnostic has been used (see [12] and references therein) measuring the line radiation (668 nm) emitted from locally puffed He (10^{19}–10^{20} atoms/s) in hydrogen discharges. The fan of 16 lines of sight (LoS) of GPI lies on the plane (r, ϕ), that is perpendicular to the main magnetic field at the edge (poloidally directed in RFPs). The LoS are 5 mm toroidally spaced and have an effective field-of view of 4 mm (both toroidally and poloidally). The bandwidth is 2 MHz. Simultaneous measurements of GPI diagnostic and Langmuir probes in another RFP device (TPE-RX) showed a good correlation between emission line and ion saturation current signals [13], proving that both diagnostics unveil the same dynamic of the turbulence.

* Corresponding author.
E-mail address: paolo.scarin@igi.cnr.it (P. Scarin).

0022-3115/$ - see front matter © 2009 Elsevier B.V. All rights reserved.
doi:10.1016/j.jnucmat.2009.01.129

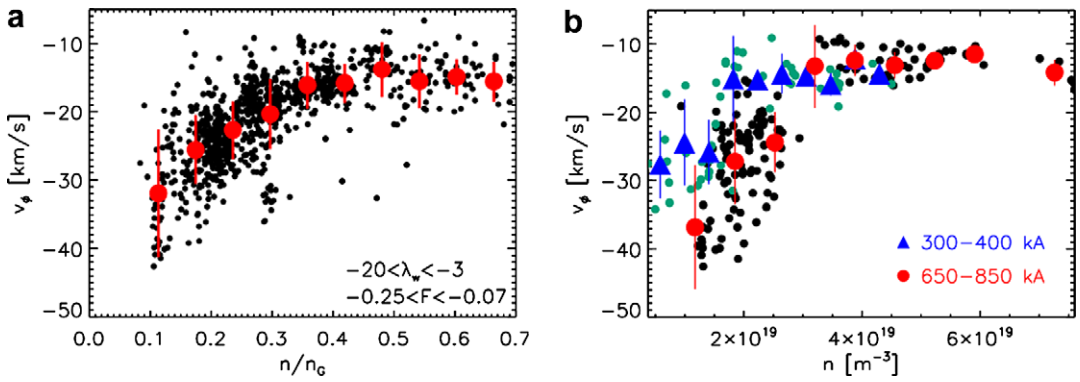

Fig. 1. (a) Scaling of toroidal velocity of emission fluctuations v_ϕ vs n/n_G; (b) scaling of v_ϕ vs n for different ranges of plasma current.

2. Cross-correlation results

We discuss experimental results by comparing discharges with different density and plasma current (quantified in terms of n/n_G), for a selected range of the reversal parameter F and of the local distance λ_w. The emission of HeI line indicates that random 'bursts' emerge from the background turbulence. Since contiguous LoS's show a similar patterns, just shifted in time, there is evidence of a toroidal propagation of these bursts in the direction opposite to plasma current, the same as the $\mathbf{E}\times\mathbf{B}$ drift flow [11,14]. The phase toroidal velocity v_ϕ of the fluctuations (from here on, for short, 'fluctuation velocity') is evaluated by one dimensional time-delay-estimation velocity technique, that infer the velocity of plasma fluctuations using the cross-correlation between spatially separated signals [15]. In Fig. 1(a) the scaling of v_ϕ vs n/n_G is shown; each black point is an average over 10 ms during the current flat-top (this same time average will be used in all the following scaling). The experimental range of $0.1 \leqslant n/n_G \leqslant 0.7$ has been divided into 10 intervals and the average values of toroidal velocity, in the corresponding data sets, have been considered (red dots); the bar in Fig. 1(a) represents the rms deviation (this kind of visualization will be used in all the following scaling). By comparing discharges with various values of n/n_G (with selected parameters $-20 \leqslant \lambda_w \leqslant -3$ mm and $-0.25 \leqslant F \leqslant -0.07$) an increase of $|v_\phi|$ at lower values is evident, a 'critical' density at $n/n_G \approx 0.35$ is observed, above which a saturation of v_ϕ at a value of about -15 km/s is found. The fluctuation velocity has been found experimentally consistent, both in direction and absolute value, with the $\mathbf{E}\times\mathbf{B}$ drift obtained from the radial gradient of plasma potential [16] and so it is often used as a fluid velocity. The trend of v_ϕ vs n/n_G is not an effect of the electron density alone but also of the plasma current. Indeed in Fig. 1(b) the scaling v_ϕ vs n for two different ranges of plasma current (300–400, 650–850 kA) is shown and the saturation of v_ϕ is obtained for different electron densities at different plasma currents.

3. Analysis of emission bursts

The high spatial resolution of the optical diagnostic gives the opportunity to study the spatial features of intermittent emission bursts and to count their number per unit of toroidal length (spatial density). The analysis is carried out using the Conditional Average technique. For each LoS we consider the fluctuations normalized to their rms values. The reference signal, against which the presence of a burst in the emission signal must be discriminated, is the intensity measured by the central chord of the fan. A characterization of burst presence at each time scale τ can be given by Local Intermittency Measure technique [17], based on the Continuous Wavelet Transform. From the simultaneous measurements of the intensity of the same burst on the 16 toroidally equidistant LoS it is possible to reconstruct the toroidal pattern of a single structure at different time scales. An estimate of the toroidal width of structures is obtained by averaging all the event patterns at each time scale within a given time window Δt and superimposing a best fit of Gaussian shape $\exp[-(x/\sigma)^2]$ on top of the obtained average pattern. In Fig. 2(a) the experimental toroidal (dots) pattern and the Gaussian fit (dashed lines) are shown for two different τ values. In general it has been found that the toroidal width $2\sigma(\tau)$ increases non-linearly with τ for fixed n/n_G [10]. The behavior of $2\sigma(\tau)$ vs n/n_G is shown in Fig. 2(b) (for two τ's) and a slight decrease of the average value with n/n_G is pointed out. These results have been obtained from discharges selected within ranges of

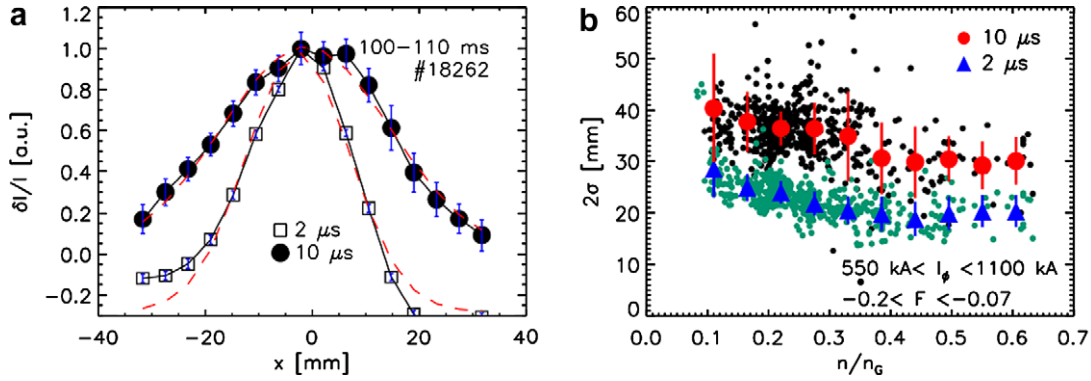

Fig. 2. (a) Toroidal patterns of intermittent structures at two different time scales; (b) scaling of toroidal pattern 2σ vs n/n_G.

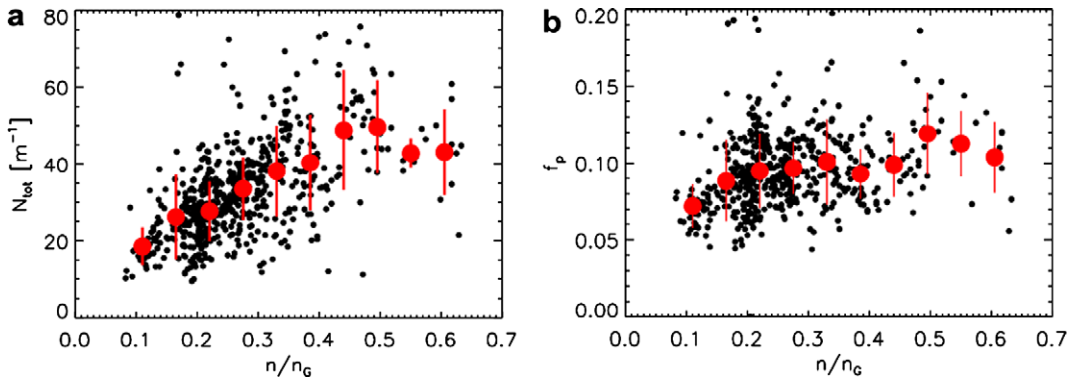

Fig. 3. (a) Scaling of total linear density of structures N_{tot} vs n/n_G; (b) packing fraction scaling f_p vs n/n_G.

plasma current and reversal parameter ($550 \leqslant I_\phi \leqslant 1100$ kA, $-0.2 \leqslant F \leqslant -0.07$). In order to understand the effect of coherent structures on the transport it is important to know, besides the width of the blobs, also their density. In RFX-mod, structures appear as filaments elongated along the poloidal direction [18]: they fill the whole field of view poloidally. Therefore, it is sufficient to count the number of structures per unit of toroidal length (from here on, for short, we will omit specifying the direction). To count the number of emission bursts per unit of length we consider their number ΔN for each time scale τ in a time window Δt, the linear density of emission structure is evaluated as $N(\tau) = \Delta N/(\Delta t \cdot v_\phi)$ at fixed τ. In order to study the global effect on the particle losses, we need the total linear density of the structures $N_{tot} = \sum_\tau N(\tau)$, by summing $N(\tau)$ over all the turbulence characteristic time scales 1 μs < τ < 10 μs. The lower limit is set by the diagnostic setup and by the turbulence' characteristic times as evaluated from its power spectrum [11]; the upper limit has been chosen empirically as well: no structures spanning times larger than this are observed and it corresponds at the characteristic frequency f^* of power spectrum from which the power-law decay begins ($f^* \approx 100$ kHz in RFX-mod). The behavior of N_{tot} vs n/n_G has been reported in Fig. 3(a) for the same discharges of Fig. 2(b): the total linear density of the structures emerging from the background turbulence increases with n/n_G in the range 0.1–0.5; at higher values the statistic is too poor to draw definite conclusions.

Another quantity that quantifies the role of the edge turbulence on the plasma transport is the structures' packing fraction f_p [8,19], estimated as the fraction of the area occupied by emission structures in the plane perpendicular to the magnetic field: $f_p = \sum_\tau \Delta N \cdot 2\sigma(\tau)\delta_r(\tau)/(\Delta t \cdot v_\phi \delta_r(\tau)) = \sum_\tau N(\tau) \cdot 2\sigma(\tau)$ where $\delta_r(\tau)$ is the radial width of coherent structures at time scale τ (numerically f_p results a fraction of the length occupied by emission structures). Smaller scale structures whose time occurrence lies within the width of the larger ones have not been considered to avoid double counting. In Fig. 3(b) f_p vs n/n_G has been reported for the same plasma shots seen in Fig. 3(a). Despite the fact that the total linear density of coherent structures increases with n/n_G, it is clear that the average packing fraction value is about constant (∼10%) for $n/n_G = 0.15$–0.45, showing that in this range the smaller scale structures can be nested into larger scale ones.

4. Diffusion of blobs' trapped plasma

Together with several affinities, there exist also some points where it is not yet clear whether RFPs and other devices are run by the same physics. One such point concerns the kind of transport associated to structures. In most Tokamaks, as well as other devices, the transport is mainly convective: single lumps of matter detach from the LCFS and, with a speed a fraction of the sound velocity, move onto the wall. In RFPs there is no such evidence; the only motion clearly diagnosed is that along the toroidal direction, which amounts to an appreciable fraction of the sound speed as well (these findings, however, are not unique to RFPs: even some Stellarators and Tokamaks [20] reported similar results). It is commonly regarded-although not unambiguously established-therefore, that the nature of transport be diffusive, consequence of the transfer of matter between structures occurring during structure-structure collisions (Horton's potential vortex theory [19]). The plasma diffusion coefficient can be separated, hence, in a part due to the plasma transported by coherent structures and another due to the background uncorrelated turbulence, usually set equal to the Bohm diffusion [8,19]. An effective diffusion coefficient D_p can be estimated in arbitrary unit as $f_p^2 \cdot u \cdot \Delta_s$ where u is the relative speed between the blobs and Δ_s their characteristic radial width [19]. In our analysis the relative speed u has been assumed to be the rms of toroidal velocity v_ϕ, $u = \mathrm{RMS}(v_\phi)$. In Fig. 4(a) the scaling of RMS(v_ϕ) vs n/n_G is shown for the same discharges seen in Fig. 2(b): the average value of RMS(v_ϕ) decreases with n/n_G and shows a saturation at about 5 km/s for $n/n_G > 0.35$. The characteristic width Δ_s of the structures has been assumed equal to the toroidal width 2σ at the higher time scale $\tau = 10$ μs. Actually, Δ_s should be taken the size of the structures along the radial direction, but we do not have available such information, while it is quite reasonable to assume that the radial and toroidal width are proportional to each other. Moreover it has been conventionally assumed $\Delta_s = 2\sigma$(@10 μs) because the larger scales give a higher effect on the diffusion coefficient D_p and also they can have nested inside smaller scales. In any case this assumption does not invalid the target of the analysis that is the study of relative behavior of D_p in different plasma conditions. The scaling of the product $f_p^2 \cdot u \cdot \Delta_s$ with n/n_G is shown in Fig. 4(b): it gives the behavior of particle diffusion from plasma driven by coherent structures. There is a large scatter of data, especially at low density, however some evidence for a slight decrease with increasing n/n_G may nonetheless be recovered. The higher dispersion of D_p data at low n/n_G values is due essentially to that of RMS(v_ϕ). At low n/n_G values the emission bursts are not strong, so the cross-correlation from different GPI signals is a little faint and the best fit that give v_ϕ is affected from such dispersion of RMS(v_ϕ) values, in any case it is possible to recover the meaning of the trends of RMS(v_ϕ) and D_p with n/n_G considering the average values over a large data base measurements. These trends can be interpreted as an increase of blob viscous damping at higher n/n_G values [6].

5. Conclusions

In RFX-mod systematic analysis of edge turbulence has been obtained with GPI diagnostic in a large set of plasma discharges.

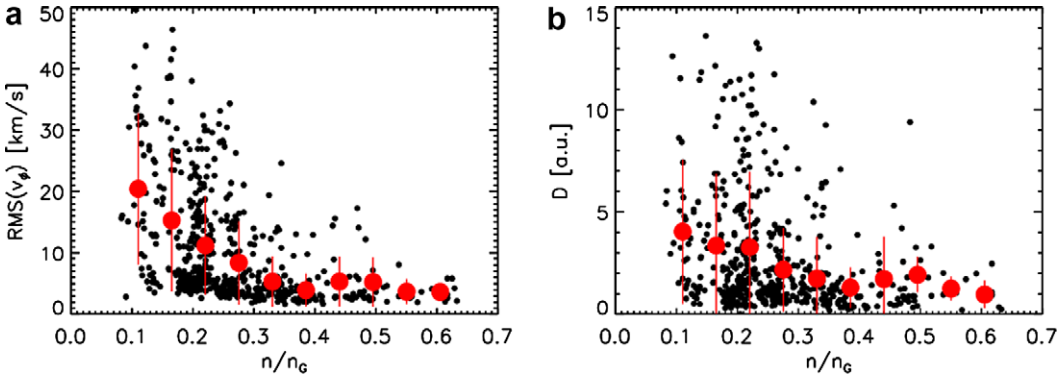

Fig. 4. Scaling of relative speed between blobs RMS(v_ϕ) vs n/n_G; (b) scaling of D_p vs n/n_G.

Average trends with n/n_G are obtained for several parameters (width, packing fraction, velocities). In this work we have focused specifically on quantifying the transport due to coherent structures, through an effective diffusion coefficient D_p. We guessed a trend with n/n_G but without unambiguous evidence. Because of its importance in the overall particle balance at the edge (with relevance for the important issue of density limits [21]), a more precise investigation of D_p is sought, as well as a clearer assessment of the precise nature of transport at the edge (i.e. if and to what extent a convective contribution should be included). To understand better the meaning of the edge transport of coherent structures one needs to measure an effective radial speed of the blobs and their radial width. Moreover to obtain a more complete view of edge transport will be useful to resolve the issue of blob creation [2]; this item will be investigate trough the measurement of the characteristic e-folding length of radial profile of plasma pressure and its comparison with the turbulence scale lengths [22].

References

[1] S.J. Zweben et al., Plasma Phys. Control. Fus. 49 (2007) S1.
[2] J.R. Myra et al., Phys. Plasmas 13 (2006) 092509;
C. Theiler et al., Phys. Plasmas 15 (2008) 042303.
[3] I.L. Terry et al., Nucl. Fus. 45 (2005) 1321.
[4] M. Greenwald, Plasma Phys. Control. Fus. 44 (2002) R27;
M. Valisa et al., in: Proceedings of the 21st IAEA Fusion Engineering Conference, Chengdu, China, 2006.
[5] J.A. Boedo et al., J. Nucl. Mater. 313–316 (2003) 813.
[6] G.Y. Antar et al., Phys. Plasmas 12 (2005) 082503.
[7] M. Farge et al., Phys. Plasmas 13 (2006) 042304;
F. Sattin et al., Plasma Phys. Control. Fus. 48 (2006) 1033.
[8] M. Spolaore et al., Phys. Rev. Lett. 93 (2004) 215003.
[9] S. Cappello, Plasma Phys. Control. Fus. 46 (2004) B313.
[10] R. Paccagnella et al., Phys. Rev. Lett. 97 (2006) 075001.
[11] P. Scarin et al., J. Nucl. Mater. 363–365 (2007) 669.
[12] G. Serianni et al., Plasma Phys. Control. Fus. 49 (2007) 2075.
[13] M. Agostini et al., Plasma Phys. Control Fus. 50 (2008) 095004.
[14] R. Cavazzana et al., Plasma Phys. Control. Fus. 49 (2007) 129.
[15] J.L. Terry et al., J. Nucl. Mater. 337–339 (2005) 322–326;
J.H. Yu et al., J. Nucl. Mater. 363–365 (2007) 728.
[16] G. Van Oost et al., Plasma Phys. Control. Fus. 45 (2003) 621–643;
V. Antoni et al., J. Nucl. Mater. 313–316 (2003) 972–975.
[17] M. Onorato et al., Phys. Rev. E 61 (2000) 1447;
V. Antoni et al., Europhys. Lett. 54 (2001) 51.
[18] M. Spolaore et al., in: Eighteenth PSI Conference, Toledo, 2008. J. Nucl. Mater. 390-391 (2009) 448.
[19] W. Horton, Y.H. Ichikawa, Chaos and Structures in Nonlinear Plasmas, World Scientific, Singapore, 1996.
[20] O. Grulke et al., Phys. Plasmas 8 (2001) 5171;
B.K. Joseph et al., Phys. Plasmas 4 (1997) 4292;
E. Martines, M. Hron, J. Stökel, Plasma Phys. Control. Fus. 44 (2002) 351.
[21] B. LaBombard et al., Phys. Plasmas 8 (2001) 2107;
M.E. Puiatti et al., Phys. Plasmas 16 (2009) 012505.
[22] K. Hallatschek, A. Zeiler, Phys. Plasmas 7 (2000) 2554.